Journal of Catalysis 270 (2010) 242–248

Contents lists available at ScienceDirect

Journal of Catalysis

journal homepage: www.elsevier.com/locate/jcat

Aromatization of hexane over Pt/KL catalyst: Role of intracrystalline diffusion on catalyst performance using isotope labeling

Khalid G. Azzam, Gary Jacobs, Wilson D. Shafer, Burtron H. Davis *

Center for Applied Energy Research, University of Kentucky, 2540 Research Park Drive, Lexington, KY 40511, USA

ARTICLE INFO

Article history:
Received 26 October 2009
Revised 22 December 2009
Accepted 1 January 2010
Available online 16 February 2010

Keywords:
Dehydrocyclization
Hexane-d_0
Hexane-d_{14}
Pt/KL
L-zeolite
Isotope effect
Diffusion

ABSTRACT

Aromatization of hexane using an equimolar mixture of C_6H_{14} and C_6D_{14} was investigated over 1%Pt/KL at 500 °C and 1 atm. There is hardly any kinetic isotope effect indicating that entry of hexane molecules into the wider lobes of the channels of L-zeolite through the narrow apertures leads to single-file hexane access to Pt^0 sites. The catalyst displayed high activity and selectivity to benzene and excellent stability at the tested conditions during hexane dehydrocyclization. It is proposed that controlling the entry of hexane into the lobes of the L-zeolite containing the active sites is the reason for the exceptional Pt/KL catalytic performance for aromatization because the narrow windows of the L-zeolite channels inhibit the occurrence of bimolecular reactions that lead to coke formation and catalyst deactivation.

1. Introduction

Catalytic reforming is an important reaction used for the production of aromatics from paraffins. The production of benzene is important, as it is a feedstock for many industrial applications in the production of drugs, plastics, synthetic rubber, and dyes. Commercially, Pt supported on chlorinated alumina containing other metallic components, such as Re [1–3], Sn [4–6], Ir [4,7,8], and/or Ge [9,10], is the catalyst commonly used for catalytic reforming. These catalysts are efficient in transforming C_7 and higher paraffins to aromatics; however, over these catalysts, the transformation of hexane to benzene proceeds with much lower selectivity [11].

In 1980, Bernard [12] reported the exceptional activity and selectivity of the non-acidic Pt/KL zeolite catalyst for the aromatization of hexane to benzene. Since that time, several hypotheses have been proposed in the literature [13–21] to explain the high activity and selectivity of the Pt/KL catalyst. Tauster et al. [14] and Derouane et al. [15] ascribed the unique feature of Pt/KL to the geometric characteristics of the catalyst. They [14,15] proposed that the structure of the catalyst orients the hexane molecule in the linear channels in such a way that it favors the C_1–C_6 closure on the Pt surface. Other authors [16–18] indicated that support microstructure does not contribute directly to the aromatization selectivity over Pt/KL catalyst and rather claimed that the excellent performance of Pt/KL is due to the role of the basic zeolite in stabilizing extremely small electron-rich Pt particles (<1 nm) of specific morphology under reaction conditions. Iglesia et al. [19,20], on the other hand, proposed that the structure of the L-zeolite helps to maintain the Pt particles inside the channels clean by preventing bimolecular reactions of hexane leading to coke formation. They [19,20] attributed the high activity and selectivity of Pt/KL to the intrinsic properties of these clean Pt particles inside the channels. Despite the different hypotheses to explain the excellent catalytic performance of the Pt/KL, it is clear that the L-zeolite plays a significant role in enhancing both the activity and selectivity of Pt for hexane dehydrocyclization; however, the reason for this enhancement is still not completely understood.

The k_H/k_D normal kinetic isotopic effect (NKIE) has been used to study the mechanism of octane dehydrocyclization over Pt/SiO_2 catalyst by using a mixture of octane-d_{18} and octane-d_0 [22–25]. In these studies, a NKIE of 3.5 ± 0.4 was found at 482 °C, indicating that the rate-limiting step involves breaking of the C–H bond. The lower reactivity of C–D bond breaking relative to C–H is due to the difference in bond energies. Similarly [26,27], the data from the competitive conversion of octane-d_{18} and octane-d_0 showed that there is a NKIE for the dehydrocyclization reaction over different catalysts (e.g., Pt/Mg(Al)O and Pt–Sn/SiO_2); however, the value ($\sim$2) was somewhat lower than that of obtained for Pt/SiO_2. Nevertheless, it is obvious from these studies that the rate-determining step is the surface reaction that involves C–H bond breaking during alkane dehydrocyclization reactions over different catalysts.

---

* Corresponding author.
E-mail address: davis@caer.uky.edu (B.H. Davis).

0021-9517/$ - see front matter © 2010 Elsevier Inc. All rights reserved.
doi:10.1016/j.jcat.2010.01.002

In a well-prepared Pt/KL catalyst, the majority of the small Pt particles are located inside the channels of the KL zeolite [28–30]. Therefore, under the actual catalytic conditions of hexane dehydrocyclization, the hexane molecules likely diffuse to the Pt active sites by Knudsen diffusion (i.e., whereby molecules frequently collide with the pore wall) prior to catalytic reaction. It is therefore possible that the entry of the hexane molecules into the channels and intracrystalline diffusion of hexane play significant roles in determining the selectivity of the dehydrocyclization reaction. The aim of this research is to determine if a NKIE exists when conducting the experiment using an equal molar ratio of hexane-d_{14} and hexane-d_0 as the feed.

2. Experimental

2.1. Catalyst preparation

A sample of potassium-exchanged zeolite LTL (Süd-Chemie, Inc.) was calcined in flowing air (100 cm^3/min) at 400 °C for 4 h. After cooling, the zeolite LTL was transferred to a glove bag filled with inert gas, carefully mixed with platinum acetylacetonate (Alfa Aesar), and loaded into a sublimation tube, sealed at one end. The other end was attached to a high vacuum system, equipped with an oil diffusion pump and capable of achieving a vacuum of $<10^{-6}$ Torr. The sublimation tube was then held at room temperature for 4 h and slowly ramped (1 °C/min) to 70, 80, 90, and then 100 °C, holding at each temperature for 1 h. Finally, the temperature was ramped to 130 °C, held for 15 min, and cooled to room temperature. Following the chemical vapor deposition (CVD) procedure, the sample was light yellow in color. To decompose the $Pt(AcAc)_2$ compound, the catalyst was then calcined at 350 °C in flowing air for 4 h. The final catalyst was light gray in color. The loading was 1%Pt by weight. Various sublimation methods for obtaining highly dispersed Pt/KL can be found in the literature, e.g., [28–37].

2.2. Catalyst characterization

Brunauer–Emmett–Teller surface area (BET SA) measurements were conducted using a Micromeritics Tri-Star system to determine whether loss of surface area occurred after loading the metal. To degas, catalyst samples were slowly heated to 160 °C under vacuum (50 mTorr) and held for 14 h. Then, the sample was transferred to the adsorption unit, and nitrogen adsorption was measured at its boiling temperature.

Hydrogen chemisorption by a temperature-programmed desorption (TPD) method was carried out using a Zeton-Altamira AMI-200 unit. The catalyst was slowly heated (1 °C/min) to either 450 °C or 500 °C in 30 cm^3/min of a 33%H_2/Ar mixture and held at either 450 °C or 500 °C for 1 h. The catalyst was then cooled in flowing hydrogen to 80 °C and purged with 25 cm^3/min of flowing argon to remove weakly bound hydrogen. The catalyst was then heated in 25 cm^3/min of flowing argon to either 450 °C or 500 °C to desorb the hydrogen, and the evolved hydrogen was monitored using a thermal conductivity detector (TCD). To calibrate the signal, ten pulses of a standard amount of hydrogen were passed into a flowing argon stream.

Diffuse reflectance infrared Fourier transform spectroscopy (DRIFTS) spectra were recorded using a Nicolet Nexus 870 spectrometer equipped with a DTGS-TEC detector. A Thermo Spectra-Tech cell capable of high pressure/high temperature operation and fitted with ZnSe windows served as the reaction chamber for in situ CO adsorption measurements. Scans were taken at a resolution of 4 to give a data spacing of 1.928 cm^{-1}. The catalyst (~40 mg) was first activated at either 450 °C or 500 °C in 75 sccm 33%H_2/He for 1 h, purged with He for 15 min, and cooled to 40 °C in 50 sccm of He flow. To probe the Pt^0 clusters, the catalyst was subjected to 50 sccm of 2%CO/He at 40 °C for 30 min. The catalyst was then purged in 50 sccm He for 20 min. Scans were recorded during CO adsorption and following the He purge. A 1%Pt/γ-Al_2O_3 (Sasol Catalox 150 alumina) catalyst, prepared by incipient wetness impregnation, served as the reference sample.

2.3. Activity test

Catalytic tests for hexane dehydrocyclization were carried out in a stainless steel fixed-bed tubular reactor (0.5 in., o.d.) under steady state conditions. Typically, the catalysts were pressed into pellets, crushed, and sieved to yield grains of 355–600 μm diameter. A 250-mg catalyst sample was packed between two layers of quartz wool. The temperature of the catalyst bed was monitored by internal thermocouples (Fe–Cr) and maintained by a temperature controller (Ω Omega CN 3251-R). The whole system was heated to 120 °C to avoid condensation of hexane. The reactor was operated under flowing H_2. Hexane-d_0 and hexane-d_{14} (Alfa Aesar, 99% purity) were added by infusion with a syringe pump (Thermo Scientific, model Orion M361) through a tee-junction located prior to the reactor. The H_2/hexane ratio was kept at 6. Prior to catalytic testing, the catalyst was reduced in H_2 at 500 °C for 15 min (temperature ramp of 4 °C/min). Reaction testing was conducted at a WHSV of 10 h^{-1} at atmospheric pressure and a temperature of 450 and 500 °C. A purge-valve was used to automatically send samples to the GC for analysis. The exit line from the purge-valve is sent to a cold trap (cooled with dry ice) to collect the products. The feed and products were analyzed using an Agilent GC (7890A) which includes a HP-PLOT/Al_2O_3 'S' deactivated capillary column to achieve product separation. Products were detected using a flame ionization detector (FID). A linear 40-min temperature ramp from 35 to 180 °C provided the means for adequate peak separation in the GC column. Due to the good separation of hexane-d_0 and hexane-d_{14} in the column (see Fig. 1), the conversions of both reactants were calculated using the FID data. The collected liquid products from the trap were analyzed using an Agilent GC (6890)–MS (5973N) to investigate the extent of H-labeled hydrogen incorporation in the deuterated hexane reactant and the extent of D incorporation in the H-labeled hexane reactant.

3. Results and discussion

The amount of hydrogen evolved from the 1%Pt/KL CVD catalyst during TPD was 51.2 and 50.5 μmol/g, respectively, for the two reduction temperatures of 450 °C and 500 °C employed. These values correspond closely to a H/Pt ratio of 2.0 (Table 1). Virtually identical results, obtained using the volumetric chemisorption approach, were reported previously [28,32] and indicate that the Pt clusters in the catalyst used in this work are extremely well-dispersed. Although H/Pt ratios above 1.0 are common in the literature [31,32,38–40] for Pt/KL catalysts, the CVD method consistently yields among the highest dispersions. Not only are

Table 1
Physical and chemical characteristics of the catalysts.

Catalyst	S_{BET} (m^2/g)	Pore volume (m^3/g)	H/Pt[a]	
KL[b]	291	0.1426	–	–
1 wt.% Pt/KL[c]	190	0.1000	2[d]	2[e]

[a] Measured by H_2 – TPD.
[b] Calcined at 400 °C.
[c] Calcined at 350 °C.
[d] Reduced in H_2 at 450 °C.
[e] Reduced in H_2 at 500 °C.

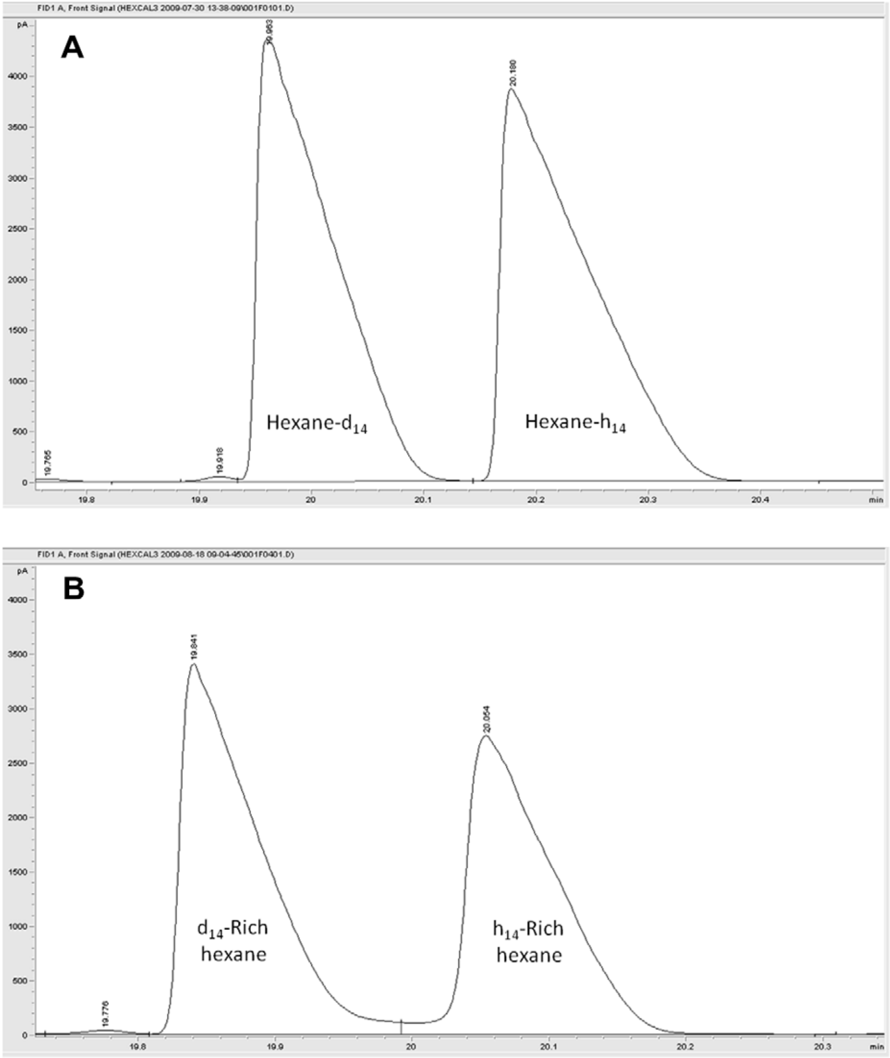

Fig. 1. FID gas chromatogram showing the efficiency of separating the hexane-H_{14} and hexane-D_{14} using the HP-PLOT/Al_2O_3 'S' deactivated capillary column, (A) before reaction and (B) after reaction.

the particles generally smaller, but since they are not clustered to form a large particle, they exhibit greater spatial separations within the zeolite pores [28].

One method to verify the likelihood that the Pt^0 clusters are mainly within the zeolite channels is to use CO as a probe and follow the evolution of Pt carbonyl species by Fourier transform infrared (FTIR) spectroscopy. These carbonyl species are formed by the disruption of only highly dispersed Pt clusters by CO; they are stabilized by a ligand effect, proposed to be due to the interaction between electron-rich zeolite O atoms, located inside the zeolite channels, and the $Pt_X(CO)_Y$ species [41,42]. That is, the basicity of the support is responsible for the ligand effect, in a similar manner that Longoni–Chini Pt-carbonyls are stabilized in solution by, for example, tertiary phosphines [43]. In agreement with this perspective, Pt particles in KL zeolite have been observed to be completely disrupted by in situ EXAFS [44]. Another view is that there is an electrostatic interaction [45], and Lane et al. [46] suggested this occurs between the potassium cation and linearly bound CO; in another perspective, an electronic effect due to electron transfer from the zeolite to small Pt particles has been postulated [40]. Fig. 2 (left, A and B) shows the evolution of Pt carbonyl species for 30 min, while Fig. 2 (right, C and D) shows a comparison after a 20-min purge in He of 1%Pt/KL CVD versus the 1%Pt/γ-Al_2O_3 reference compound. The majority of bands for 1%Pt/KL CVD are positioned at wave numbers much lower than the linear ν(CO) band observed for the typical 1%Pt/γ-Al_2O_3 catalyst. Furthermore, the low-wave number bands appear at discrete positions (e.g., for the catalyst reduced at 500 °C prior to CO adsorption, the bands are positioned at 2049, 2035, 2030, 2014, 2006, with a series of shoulders from 2000 to 1915 cm^{-1}), suggesting that they likely correspond to $Pt_X(CO)_Y$ species stabilized by the L-zeolite support.

Although the DRIFTS results of adsorbed CO indicate that a high fraction of Pt resides inside the channels (Pt carbonyl bands ranging from 2049 cm^{-1} to 1915 cm^{-1}), there is also a shoulder present at 2067 cm^{-1} for CO adsorbed on larger Pt metal crystallites. These particles are likely large enough to block the narrow window of the L-zeolite and therefore completely cut off reactant access to a fraction of the channels. The DRIFTS spectra were fitted using a least squares fitting procedure with Gaussian peaks. Two Gaussian peaks were used to define the ν(CO) of linearly bound CO on larger Pt crystallites (2067 cm^{-1} +), and five Gaussian peaks were used to define the ν(CO) bands of $Pt_X(CO)_Y$ species stabilized by the KL zeolite (<2067 cm^{-1}), as depicted in Fig. 2E and F. Approximately 20% of the linear stretching bands correspond to those assigned to CO adsorbed on larger Pt crystallites. This is consistent with a decrease

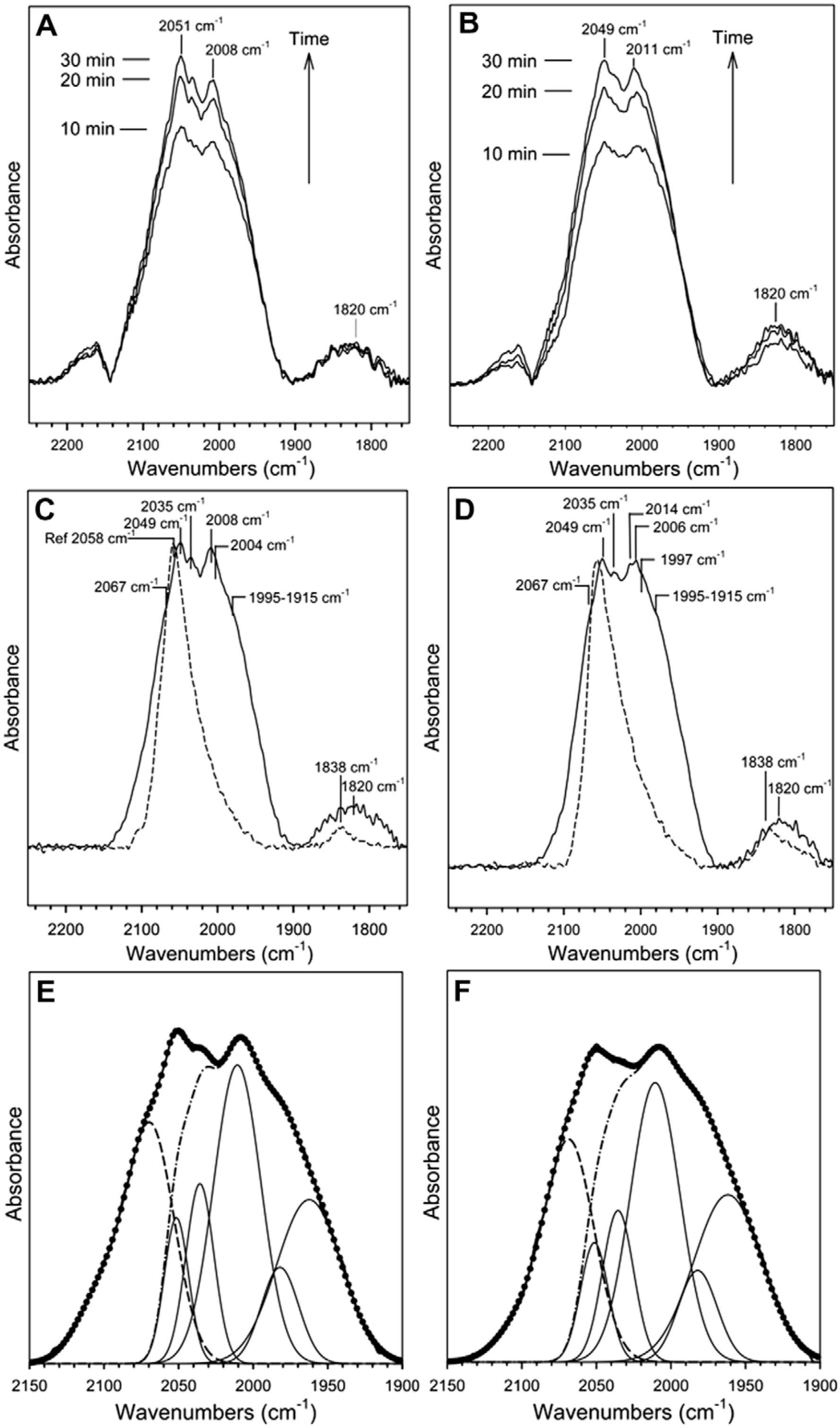

Fig. 2. (Left) CO adsorption over 1%Pt/KL using 50 ccm of 2%CO/He at 40 °C after reduction at (A) 450 °C or (B) 500 °C in 75 ccm of 33%H_2/He and cooling in 50 ccm He. (Right) Corresponding spectra (C and D) after a 20 min 50 ccm He purge for (solid line) 1%Pt/KL and (dashed line) 1%Pt/γ-Al_2O_3. Note the height of the ν(CO) band for Pt/alumina was multiplied by 0.65 (450 °C data) and 0.45 (500 °C data) to normalize. Gaussian fitting of ν(CO) for linearly bound CO (dashed, two components) and ν(CO) in Pt-carbonyls (dash-dotted, five components) for (E) 450 °C and (F) 500 °C H_2-reduced catalysts following CO adsorption at 40 °C and He purge.

in the BET surface area and pore volume by a fraction of ~1/3 (see Table 1) observed after Pt addition and calcination relative to KL zeolite alone. Nevertheless, DRIFTS results demonstrate that the majority of Pt is small enough, and in sufficient contact with the KL zeolite channels, as to be converted to KL support-stabilized Pt carbonyl species upon CO adsorption (~80% of the linear ν(CO) bands). As mentioned previously, adequate basicity is a requirement in the formation of Pt carbonyl species and can only be provided in this case by the KL zeolite. From the hydrogen chemisorption and DRIFTS results, one can conclude that the majority of Pt clusters are ultra-well-dispersed and located within the channels of the L-zeolite.

Table 2
Dehydrocyclization of equimolar mixture of hexane-d_0 and hexane-d_{14} over 1%Pt/KL catalyst at 500 °C, 1 atm, WHSV = 10 h^{-1}, H_2/hexane ratio of 6.

Time (h)	Conversion (%)		Conversion-h_{14}/conversion-d_{14}
	d_0	d_{14}	
0.25	43	38	1.13
1.75	37	30	1.23
2.50	38	29	1.31
4.00	43	37	1.16
5.50	45	38	1.18
Average	41.2	34.4	1.2
St. Dev.	3.5	4.5	0.1

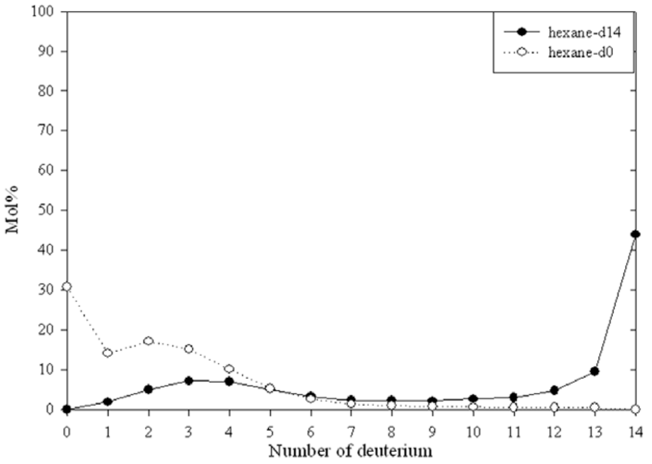

Fig. 3. Deuterium distribution in the recovered hexane (equimolar feed of hexane-d_{14}/hexane-d_0) after the dehydrocyclization reaction over 1%Pt/KL at 450 °C, 1 atm, WHSV = 10 h^{-1}, H_2/hexane ratio of 6.

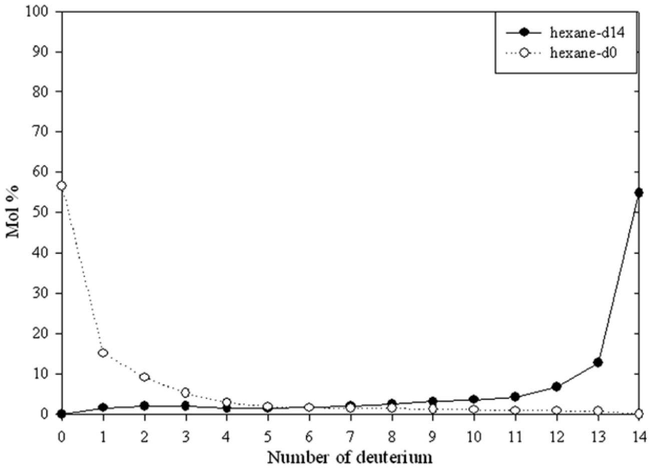

Fig. 4. Deuterium distribution in the recovered hexane (equimolar feed of hexane-d_{14}/hexane-d_0) after the dehydrocyclization reaction over 1%Pt/KL at 300 °C, 1 atm, WHSV = 10 h^{-1}, H_2/hexane ratio of 6.

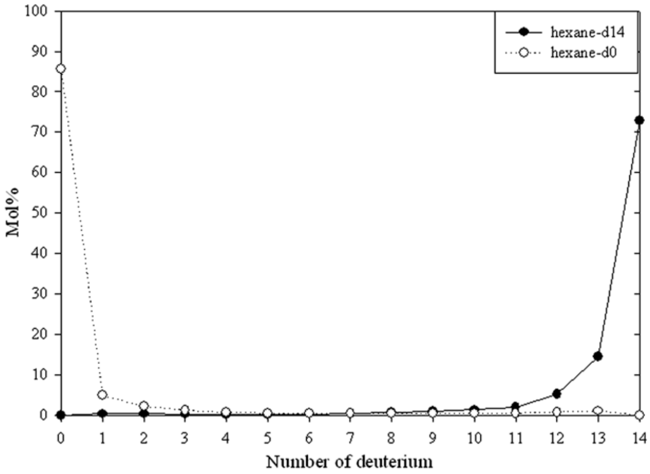

Fig. 5. Deuterium distribution in the recovered hexane (equimolar feed of hexane-d_{14}/hexane-d_0) after the dehydrocyclization reaction over 1%Pt/KL at 500 °C, 1 atm, WHSV = 10 h^{-1}, H_2/hexane ratio of 6.

Table 2 shows the relative conversions of the equimolar C_6H_{14} and C_6D_{14} over the 1%Pt/KL versus time on-stream at 500 °C and atmospheric pressure. Over the tested period (5.5 h), the catalyst showed good stability with average conversion of 41% and 34% for C_6H_{14} and C_6D_{14}, respectively, and an average calculated NKIE (k_H/k_D) of 1.2 ± 0.1. The carbon balance was good in all analyses with a value of 1 ± 0.07. The results indicate that there is hardly any NKIE detected for the conversion of an equimolar mixture of C_6H_{14} and C_6D_{14} on the tested catalyst (1%Pt/KL). It is well established in the literature [22–25,47,48] that (i) the adsorption of a mixture of alkanes–alkanes or alkanes–cycloalkanes is competitive and irreversible during the dehydrocyclization reaction over Pt catalysts at temperatures at or above ca. 480 °C and 1 atm and (ii) a reaction that exhibits a significant decrease in conversion when switching from a C–H label to the C–D label in the reactant involves breaking of that C–H bond in the rate-limiting step due to the NKIE arising from the difference in bond energy [23,49,50]. Irreversible adsorption has been shown to be temperature dependent [22,47]. Thus, at 300 °C, adsorption is not rate limiting so that the cycloalkane is converted much more rapidly than the alkane [17,43]. Furthermore, it was observed that there was more H–D exchange in the unconverted reactant following exposure to the catalyst at the low-temperature condition [22,47,48]. In this study, H–D exchange in the unconverted hexane when the reaction was conducted at 450 °C (Fig. 3) or at 300 °C (Fig. 4) was more pronounced compared with the 500 °C condition (Fig. 5). The occurrence of H–D exchange at 300 °C or at 450 °C and the lack of exchange at 500 °C indicate a change from reversible adsorption at lower temperature to irreversible adsorption at 500 °C, the typical temperature for aromatization over Pt/KL.

Surprisingly, H–D exchange at 450 °C occurred to a greater extent than at 300 °C, and the H–D exchange in the unreacted hexane at 300 °C is far from equilibrium. It was reported by Shi and Davis [22], based on their observation of H–D exchange in octane over Pt/SiO_2 catalyst using an octane/methylcyclohexane mixture, that the rate of isotope exchange and the depth of exchange increased as the temperature decreased. Our observation on H–D exchange at 300 and 450 °C over the Pt/KL catalyst indicate that this is not the case for the microporous Pt/KL catalyst. It is well established that in a well-prepared Pt/KL catalyst, as confirmed by our hydrogen chemisorption and DRIFTS results, the active sites reside inside the channels of the L-zeolite [16,28,29,51]. Considering the orders of magnitudes in pore diameter of the nanoporous materials, this means that Pt sites in microporous (0.7–1.1 nm) Pt/KL will exhibit less open contact relative to the mesoporous catalysts like Pt/SiO_2 (∼27 nm for PQ CS-2133 silica). Thus, since the hexane molecules must enter and diffuse through the channels of the L-zeolite to reach the Pt active sites in order for H–D exchange to occur, a higher fraction of hexane molecules will not access the Pt sites if diffusion of hexane is slow. Therefore, if at lower temperatures the diffusion of hexane molecules is the rate-limiting step of H–D exchange, then at higher temperature (450 °C) the diffusion of the hexane molecules through the channels of the L-zeolite will be faster than at 300 °C and hence more H–D exchange can occur, in agreement with our observations. Another possibility that could explain the finding that a higher rate of exchange occurs at 450 °C is due to the faster kinetics of the surface reaction. However, in previous studies by Shi and Davis [22], the exchange achieved equilibrium over Pt/SiO_2 catalyst even at 300 °C; thus, the previous explanation regarding diffusion control appears to be valid.

The lack of a NKIE at 500 °C (see Table 2) reveals that the channels of the L-zeolite play a significant role in controlling the entry of hexane molecules to the active surface sites; these are located on the Pt^0 crystallites, which reside inside the lobes of the uni-axial channels. In contrast to the non-microporous catalysts (e.g., Pt/SiO_2) in which irreversible reactant adsorption is reported to be the rate-determining step based on the lack of H/D exchange in the recovered reactants and significant NKIE [22–26], the entry into the pore opening and intracrystalline diffusion of hexane seems to be the slowest step in the dehydrocyclization reaction over Pt/KL. If this was not the case, a more pronounced NKIE should be observed. Indeed, the adsorption of hexane-d_0 or hexane-d_{14} is also irreversible in our case based on the lack of H/D exchange of the recovered reactants at 500 °C shown in Fig. 5. It is obvious from Fig. 5 that there is very little H incorporated into hexane-d_{14}, and this also applies to hexane-h_{14} where there is little D incorporation observed. This means that almost all the reactants that are adsorbed on Pt sites complete the reaction to final products [23]. However, based on the fact that there is no NKIE when using the equimolar C_6H_{14} and C_6D_{14} mixture over Pt/KL, the entry of hexane into the pore channel and diffusion of the hexane molecules to Pt sites within the channels of the Pt/KL catalyst seem to determine the selectivity for, or absence of, H–D exchange in the reactants. Moreover, the L-zeolite is reported to have uni-axial pores with a narrow 0.7-nm aperture leading to cavities of about 1.1 nm in diameter [52], and the average diameter of hexane molecule is about 0.454 nm [53]. Comparing the diameter of the aperture of pores and the diameter of hexane molecules, one can expect that hexane enters and diffuses on a single-file basis (i.e., one-by-one). Therefore, based on our hexane isotope distribution data and the size characteristics of hexane molecules versus the size of the narrow windows of the L-zeolite channels, we conclude that hexane dehydrocyclization over Pt/KL is controlled by the probability of reactant entry into the wider lobes of the L-zeolite channels via the narrow apertures. Since the concentration of C_6H_{14} and C_6D_{14} is equal, the probability of entry into each narrow pore opening is essentially identical and thus equal to unity, and this is nearly the ratio that is obtained experimentally. One cannot rule out a slight steric effect due to the presence of the larger D atoms.

Fig. 6 shows the product selectivity of Pt/KL to benzene versus time on-stream at 500 °C and 1 atm. Over a period of a 5.5 h of testing, the selectivity to benzene product is constant at about 70%. It is obvious from the conversion and selectivity data that the catalyst has superior activity, stability, and selectivity to benzene when Pt/KL catalyst is prepared by the CVD procedure, in agreement with the previous findings of Mielczarski et al. [16], Jacobs et al. [28,29], and Dossi et al. [54]. The authors found that using CVD methods for catalyst preparation resulted in better catalytic performance for Pt/KL than when prepared by ion exchange (IE) or incipient wetness impregnation (IWI) methods. This is because the CVD method results in a majority of ultra-tiny Pt clusters present inside the L-zeolite channels rather than external to the zeolite or in close proximity to each other at the pore mouth (i.e., resulting in significant agglomeration and noticeable initial deactivation trend). This also agrees with our hydrogen chemisorption and DRIFTS results which show that the majority of Pt clusters are well-dispersed and located within the channels of the L-zeolite. The location of highly dispersed Pt clusters inside the channels is believed to prevent Pt sintering (i.e., the narrow windows provide a kinetic barrier to Pt mobility) and suppress carbon deposition (i.e., by inhibiting bimolecular reaction pathways that lead to coking [19,20,28,29,55]).

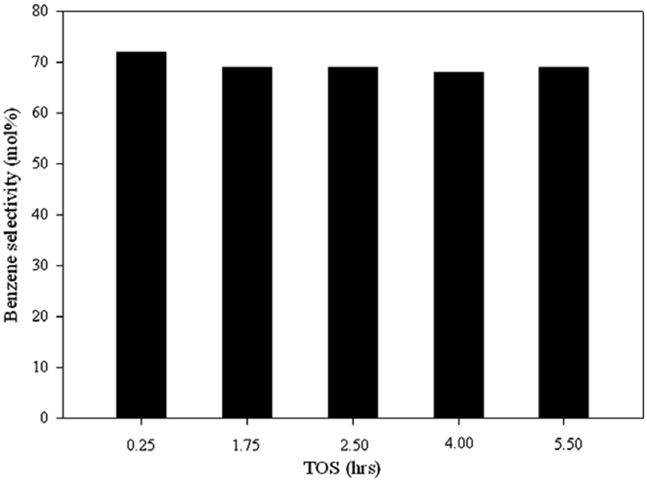

Fig. 6. Benzene selectivity vs. time on-stream obtained from the dehydrocyclization of equimolar mixture of hexane-d_0 and hexane-d_{14} over 1%Pt/KL catalyst at 500 °C, 1 atm, WHSV = 10 h^{-1}, H_2/hexane ratio of 6.

The observed results in this study, including the lack of NKIE at 500 °C when using an equimolar of C_6H_{14} and C_6D_{14} over Pt/KL CVD catalyst, the enhanced catalyst stability relative to other preparation methods, and the excellent dehydrocyclization activity and selectivity to benzene are consistent with the hypothesis of Iglesia et al. [19,20] that an important role of L-zeolite is to help maintain the Pt particles inside the channels clean by preventing bimolecular reaction pathways from occurring [19,20]. We propose based on the kinetic isotopic effect study that the dehydrocyclization reaction over Pt/KL catalyst is controlled by the entry of hexane molecules into the wider lobes of the L-zeolite where the Pt^0 active sites reside. That is, in contrast to non-microporous-supported Pt catalysts, the tiny windows of the L-zeolite channels allow hexane to pass through one-by-one to the larger lobes containing the Pt clusters. This in turn hinders the bimolecular reactions that lead to coke formation and thus prevents catalyst deactivation.

4. Conclusions

Hydrogen chemisorption and DRIFTS revealed that the majority of Pt clusters are ultra-tiny and well-dispersed within the channels of L-zeolite when the catalyst was prepared using the CVD method. There is hardly any kinetic isotope effect for the conversion of an equimolar mixture of C_6H_{14} and C_6D_{14} on 1%Pt/KL catalyst at 500 °C and 1 atm, indicating that the dehydrocyclization reaction of hexane over Pt/KL is controlled by hexane entry into the wider lobes of the L-zeolite channels where the Pt clusters reside. In contrast with non-microporous-supported Pt catalysts, the tiny windows of the L-zeolite channels allow hexane to pass through one-by-one to the larger lobes containing the Pt clusters. This controlled diffusion of hexane inside the channels seems to be the reason for the high stability and selectivity of the catalyst, most likely because it inhibits the bimolecular reactions that lead to coke formation and catalyst deactivation, in agreement with the earlier hypothesis of Iglesia.

References

[1] H.E. Kluksdahl, US Patent 3,415,737, Chevron, 1968.
[2] V.A. Mazzieri, J.M. Grau, C.R. Vera, J.C. Yori, J.M. Parera, C.L. Piec, Catal. Today 107–108 (2005) 643.
[3] N. Viswanadham, R. Kamble, A. Sharma, M. Kumar, A.K. Saxena, J. Mol. Catal. A: Chem. 282 (2008) 74.
[4] F. Epron, C. Carnevillier, P. Marécot, Appl. Catal. A: Gen. 295 (2005) 157.
[5] B.H. Davis, US Patent 3,840,475, 1974.
[6] F.M. Dautzenberg, J.N. Helle, P. Biloen, W.M.H. Sachtler, J. Catal. 63 (1980) 119.
[7] J.H. Sinfelt, US Patent 3,953,368, Exxon, 1976.
[8] C. Carnevillier, F. Epron, P. Marecot, Appl. Catal. A: Gen. 275 (2004) 25.
[9] V.A. Mazzieri, C.L. Pieck, C.R. Vera, J.C. Yori, J.M. Grau, Appl. Catal. A: Gen. 353 (2009) 93.
[10] K.R. McCallister, T.P. O'Neal, French Patent 2 078 056, UOP, 1971.
[11] N.K. Mal, M. Sasidharan, M. Matsukata, S. Sivasanker, A.V. Ramasawamy, Stud. Surf. Sci. Catal. 154 (2004) 2403.
[12] J.R. Bernard, in: Proceedings of the 5th International Conference, Heyen, London, 1980, p. 686.
[13] R.J. Davis, Heterog. Chem. Rev. 1 (1) (1994) 41.
[14] S.J. Tauster, J.J. Steger, J. Catal. 125 (1990) 387.
[15] E.G. Derouane, D.J. Vanderveken, Appl. Catal. 45 (1988) 15.
[16] E. Mielczarski, S.B. Hong, R.J. Davis, M.E. Davis, J. Catal. 134 (1992) 359.
[17] P.V. Menacherry, G.L. Haller, J. Catal. 177 (1998) 175.
[18] W. Han, A.B. Kooh, R.F. Hicks, Catal. Lett. 18 (1993) 219.
[19] E. Iglesia, J.E. Baumgartner, G.D. Meitzner, Stud. Surf. Sci. Catal. 75 (1993) 2353.
[20] E. Iglesia, J.E. Baumgartner, Stud. Surf. Sci. Catal. 75 (1993) 993.
[21] R.L. Jacobson, M.E. Kluksdahl, C.S. McCoy, API Proc. Div. Refin. 49 (1969) 504.
[22] B. Shi, B.H. Davis, J. Catal. 147 (1994) 38.
[23] B. Shi, B.H. Davis, Stud. Surf. Sci. Catal. 101 (1996) 1145.
[24] B. Shi, B.H. Davis, J. Catal. 168 (1997) 129.
[25] B. Shi, B.H. Davis, J. Catal. 162 (1996) 134.
[26] Y. Wang, B. Shi, R.D. Guthrie, B.H. Davis, J. Catal. 170 (1997) 89.
[27] B. Shi, B.H. Davis, J. Catal. 157 (1995) 626.
[28] G. Jacobs, W.E. Alvarez, D.E. Resasco, Appl. Catal. A: Gen. 206 (2001) 267.
[29] G. Jacobs, F. Ghadiali, A. Pisanu, A. Borgna, W.E. Alvarez, D.E. Resasco, Appl. Catal. A 188 (1999) 79.
[30] E.W. Berg, F.R. Hartlage, J. Anal. Chim. Acta 33 (1965) 173.
[31] E. Mielczarski, S.B. Hong, M.E. Davis, J. Catal. 134 (1992) 349 and 359.
[32] M. Ballatreccia, R. Zanoni, C. Dossi, R. Psaro, S. Recchia, G. Vlaic, J. Chem. Soc. Faraday Trans. 91 (1995) 2045.
[33] C. Dossi, R. Psaro, R. Zanoni, J. Catal. 159 (1996) 435.
[34] G. Jacobs, F. Ghadiali, A. Pisanu, C.L. Padro, A. Borgna, W.E. Alvarez, D.E. Resasco, J. Catal. 191 (2000) 116.
[35] D.E. Resasco, C.L. Padro, G. Jacobs, H.-Y. Liu, U.S. Patents 6,063,724, 6,096,193, and 6,096,675.
[36] D.B. Tiedtke, T.-T.P. Cheung, D.E. Resasco, G. Jacobs, U.S. Patent 6,406,614.
[37] S. Jongpatiwut, P. Sackamduang, T. Rirksomboon, S. Osuwan, D.E. Resasco, J. Catal. 218 (2003) 1.
[38] F. Ghadiali, G. Jacobs, A. Pisanu, A. Borgna, W.E. Alvarez, D.E. Resasco, Stud. Surf. Sci. Catal. 130 (2000) 2537.
[39] B.J. McHugh, G. Larsen, G.L. Haller, J. Phys. Chem. 94 (1990) 8621.
[40] G. Larsen, G.L. Haller, Catal. Lett. 3 (1989) 103.
[41] A. Yu Stakheev, E.S. Shpiro, N.I. Jaeger, G. Schulz-Ekloff, Catal. Lett. 34 (1995) 293.
[42] A. Yu Stakheev, E.S. Shpiro, N.I. Jaeger, G. Schulz-Ekloff, Stud. Surf. Sci. Catal. 98 (1995) 108.
[43] P. Chini, G. Longoni, J. Chem. Soc. A: Inorg. Phys. Theor. 9 (1970) 1524.
[44] B.L. Mojet, J.T. Miller, D.C. Koningsberger, J. Phys. Chem. B 103 (1999) 2724.
[45] T. Fukunaga, V. Ponec, Appl. Catal. A 154 (1997) 207.
[46] G.S. Lane, J.T. Miller, F.S. Modica, M.K. Barr, J. Catal. 141 (1993) 465.
[47] B.H. Davis, Catal. Today 53 (1999) 443.
[48] B.H. Davis, J. Catal. 23 (1971) 365.
[49] H.A. Dabbagh, T.S. Huang, B. Franzus, B.H. Davis, Tetrahedron 47 (1991) 949.
[50] A. Ozaki, Isotopic Studies of Heterogeneous Catalysis, Academic Press, New York, NY, 1977.
[51] I. Manninger, Z. Zhan, X.L. Xu, Z. Paàl, J. Mol. Catal. 66 (1991) 223.
[52] Y. Sig Ko, W. Seung Ahn, Bull. Korean Chem. Soc. 20 (1999) 1.
[53] F. Jimenez-Cruz, G.C. Laredo, Fuel 83 (2004) 2183.
[54] C. Dossi, R. Psaro, A. Bartsch, A. Fusi, L. Sordelli, R. Ugo, M. Bellatreccia, R. Zanoni, G. Vlaic, J. Catal. 146 (1994) 377.
[55] G. Jacobs, C.L. Padro, D.E. Resasco, J. Catal. 179 (1998) 43.